



ELSEVIER

Available online at [www.sciencedirect.com](http://www.sciencedirect.com)

SCIENCE @ DIRECT®

Geomorphology 52 (2003) 165–180

GEOMORPHOLOGY

[www.elsevier.com/locate/geomorph](http://www.elsevier.com/locate/geomorph)

# Downstream hydraulic geometry and channel adjustment during a flood along an ephemeral, arid-region drainage

David M. Merritt<sup>a</sup>, Ellen E. Wohl<sup>b,\*</sup>

<sup>a</sup>*Stream Ecology Laboratory, Department of Biology, Colorado State University, Fort Collins, CO 80523, USA*

<sup>b</sup>*Department of Earth Resources, Colorado State University, Fort Collins, CO 80523, USA*

Received 12 November 2001; received in revised form 9 June 2002; accepted 7 August 2002

## Abstract

In September 1997, a dissipating tropical storm caused a flood with an estimated maximum discharge of 240 m<sup>3</sup>/s along Yuma Wash, an ephemeral braided system draining 186 km<sup>2</sup> in southwest Arizona. Older high-water marks that record a flood peak of 1280 m<sup>3</sup>/s provide a reasonable estimate for the probable maximum flood along the wash. Detailed channel cross-sectional surveys during 1995 and again in 1998, <6 months after the 1997 flood, facilitated examination of downstream hydraulic geometry and channel adjustment during the flood. Channel width increased substantially downstream (exponent of 0.78), presumably because of low bank resistance, whereas hydraulic depth and velocity had modest downstream increases (0.15 and 0.14, respectively). Channel aggradation generally occurred along wider, braided reaches; moreover, degradation occurred in narrow reaches with fewer channels. Aggradation and degradation also appeared to be governed by a threshold relationship between flow depth and vegetated bars. Degradation occurred where flow was confined within a channel or subchannel. At discharges sufficiently high to overtop vegetated bars, greater roughness facilitated sediment deposition and channels aggraded. A discriminant function correctly classified nearly 90% of the cross-sections as scoured or filled using a single hydraulic variable, maximum depth of flow during the dissipating tropical storm.

© 2002 Elsevier Science B.V. All rights reserved.

*Keywords:* Braided channel; Discriminant analysis; Ephemeral channel; Flood; Hurricane Nora; Hydraulic geometry; Threshold response

## 1. Introduction

Previous studies of downstream hydraulic geometry relations for some ephemeral arid-region rivers in the southwest US suggest that increase of downstream rates are greater for width and velocity and

lesser for depth than average values for rivers worldwide (Leopold et al., 1964; Wolman and Gerson, 1978; Knighton, 1998) (Table 1). The differences in rate of change in width have been attributed to a flashier discharge regime, relatively high peak flows, and large volumes of sand transport, which tend to promote the formation of wider channels (Osterkamp, 1980) in ephemeral systems. Slightly more rapid downstream increases in velocity have been attributed to downstream increase in suspended sediment concentration and consequent damping of turbulence

\* Corresponding author. Tel.: +1-970-491-5298; fax: +1-970-491-6307.

E-mail address: [ellenw@cnr.colostate.edu](mailto:ellenw@cnr.colostate.edu) (E.E. Wohl).

Table 1

Downstream hydraulic geometry exponents at bankfull or near-bankfull discharge (after Leopold and Miller, 1956; Leopold et al., 1964; Park, 1977)

	Width	Depth	Velocity
Worldwide range	0.03–0.89	0.09–0.70	–0.51–0.75
Arid regions	0.5–0.63	0.2–0.3	0.17–0.20
Gravel bed (ephemeral and perennial)	0.45–0.55	0.33–0.42	0.08–0.20
Average value	0.5	0.4	0.1
Yuma Wash	0.78	0.15	0.14

(Leopold and Miller, 1956). Studies of downstream hydraulic geometry along channels in other arid regions indicate that channel width may: decrease downstream (Mabbutt, 1977; Dunkerley, 1992; Tooth, 1999a,b); approach a fairly universal asymptote value of 100–200 m once catchment area exceeds approximately 50 km<sup>2</sup> (Wolman and Gerson, 1978); or have oscillations superimposed on an overall downstream increase in width of the valley train (Thornes, 1977). These differing downstream trends have been explained as resulting from exterior versus interior drainage, differing rates of transmission loss, presence or absence of riparian vegetation, and differences in effective storm size and percent contributing area (Tooth, 2000). Existing case studies are not yet sufficient to formulate general rules describing downstream hydraulic geometry of arid-region channels as a function of potential control variables.

Tooth (2000) noted a tendency to regard dryland channels as being non- or disequilibrium systems, with transient behavior as the norm rather than the exception, and the morphology being a result of a continually changing relationship between form and process. This arises from the recognition that channel adjustment along ephemeral rivers is inherently an episodic process because of the episodicity of flow. Various investigators have examined the importance of flood magnitude and frequency in this adjustment (Wolman and Gerson, 1978; Graf, 1983b; Begin and Inbar, 1984; Kresan, 1988; Reid and Laronne, 1995). Graf's (1983a, 1988b) studies of dryland channels in the southwest US have documented decadal- to centuries-long episodes of moderate floods and channel aggradation, alternating with episodes of large floods and channel erosion. Kochel (1988) identified flashy hydrographs, steep gradients, coarse bed load, and

channel geometries conducive to highly turbulent flow as among the characteristics of channels dominated by high magnitude floods, which sufficiently exceed the threshold of channel-boundary resistance to cause significant erosion. These characteristics are present along many ephemeral rivers. The consensus is that these ephemeral rivers are highly sensitive to the effects of large floods because of lower channel-boundary resistance and a high ratio of small to large floods (Graf, 1988a; Tooth, 2000). However, Tooth and Nanson (2000) describe ephemeral channels in central Australia which have a long duration of floods with moderate to low unit stream power and high boundary resistance resulting from indurated terraces, cohesive sediments, and vegetation. These channels are stable, and have strong correlations between form and process variables, suggesting that the channels are better described as displaying equilibrium. Tooth and Nanson (2000) conclude that dryland rivers may be equilibrium or nonequilibrium systems, depending on drainage area, gradient, flood duration, unit stream power, channel confinement, sediment cohesion, and bank strength.

Channel adjustment has also been examined in terms of spatial controls such as boundary resistance or valley geometry (Baker, 1977; Wohl et al., 1994). As might be expected, more resistant boundaries and steep, narrow geometries tend to promote erosion of bed alluvium at the thalweg; whereas erodible boundaries and lower gradient-wide valleys promote bed deposition. However, the influence of larger scale substrate and geometry may be of secondary importance where patterns of vegetation strongly influence hydraulic roughness, substrate stability, and thus channel adjustment (Graf, 1978; Graeme and Dunkerley, 1993; Tooth and Nanson, 1999).

In this paper, we document and interpret the downstream hydraulic geometry relations and channel adjustment during a moderate flood along Yuma Wash in southwest Arizona. Yuma Wash is an ungagged ephemeral channel network for which direct measurements of downstream hydraulic geometry do not exist. However, the completion of channel surveys shortly before and after a flood produced by a dissipating tropical storm allowed us to (i) use evidence of peak stage during the flood to estimate peak discharge associated with the storm; (ii) document downstream hydraulic geometry during the flood; and (iii) analyze

correlations between channel change and potential control variables at the cross-sectional, reach, and basin scales. Yuma Wash may be taken as representative of ephemeral streams throughout the lower Colorado River basin because the wash shares with other streams in the region characteristics such as an externally drained channel with a braided planform, a flashy hydrograph, and a sand and gravel bed with some lateral bedrock control and riparian vegetation.

## 2. Study area

Yuma Wash is an ephemeral channel with a sand and gravel bed draining 186 km<sup>2</sup> in southwest Arizona (Fig. 1). Although the channel is formed primarily in alluvium, discontinuous bedrock outcrops along the valley walls are more common in the upper reaches. The drainage basin is bordered to the north

and west by Tertiary andesites in the Trigo and Chocolate mountains. Minor exposures of Mesozoic schists and Quaternary basalt occur along the valley walls in the middle and lower reaches of the basin (Wilson, 1960). The basin drains south at approximately 27 km from the Mohave Peak (427-m elevation) to the Colorado River (56-m elevation).

The region receives a total annual average rainfall of 93 mm (NOAA, 1998) from convective thunderstorms, frontal systems, and dissipating tropical storms. A majority of the summer rainfall comes from isolated convective storms that cause localized flash flooding. More extensive floods are likely to result from tropical storms during the autumn months, the effects of which are the focus of this paper.

Hurricane Nora entered the US near the California–Arizona border on 25 September 1997. The hurricane produced 64% of the total 1997 precipitation in Yuma Wash during a period of 10 h on 25

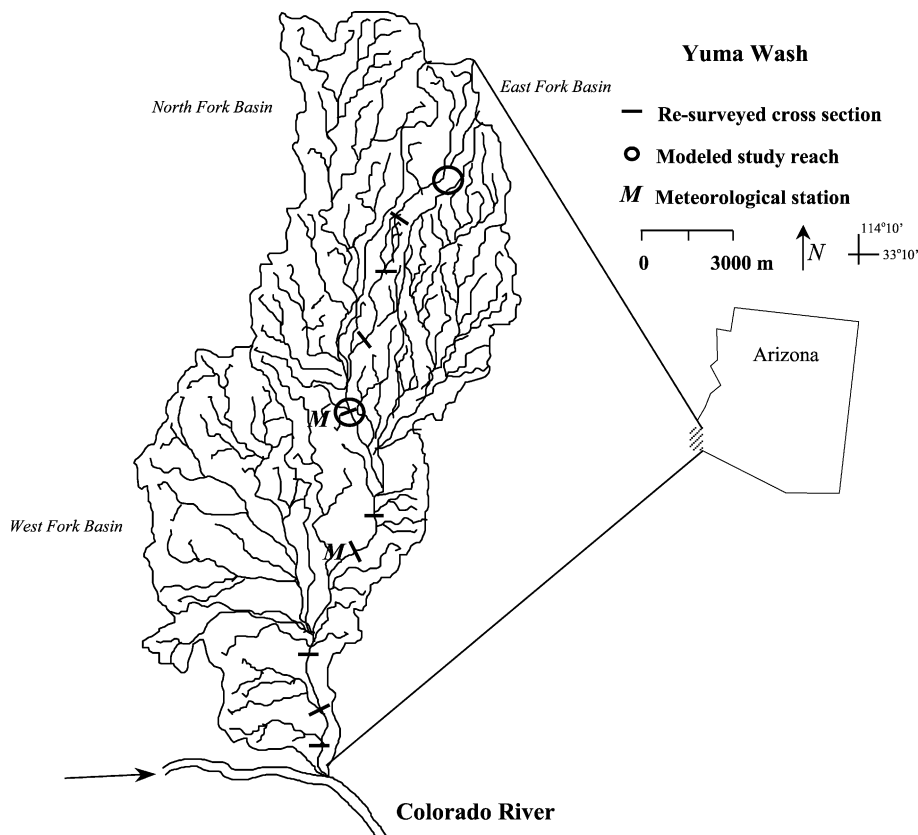


Fig. 1. Location map of Yuma Wash, indicating sites of resurveyed cross-sections, remote weather stations, and hydraulic modeling reaches.

September. Precipitation associated with the storm was recorded at two remote weather stations in Yuma Wash. Thirty-one millimeters of precipitation fell over a period of 10 h on 25 September, with a maximum intensity of 9 mm/h. This was preceded by 22 mm of precipitation on 5 September and 26 mm on 14 September, which likely produced high antecedent soil moisture at the time of Hurricane Nora. Because of the high spatial variability of precipitation in the vicinity of Yuma Wash and the limited number of long-term weather stations in the area, calculations of the recurrence intervals of storms of various magnitudes are approximations. Daily total precipitation recorded at the Yuma Proving Ground weather station, located 21 km south of Yuma Wash, equaled or exceeded the total precipitation recorded during Hurricane Nora 13 times over the period of record (1958–1997; NOAA, 1998). The largest storm on record occurred in 1972 and was nearly three times the magnitude of Hurricane Nora. These records indicate that the recurrence interval of a storm equal to the magnitude of the Hurricane Nora event is approximately every 3 years for the region. However, the large spatial extent of the rainfall associated with Hurricane Nora created a larger contributing area within Yuma Wash than is likely associated with many of the other rain events recorded at nearby weather

stations. The resulting flood along Yuma Wash is thus likely to have a much longer recurrence interval than 3 years because of spatial variability in precipitation. Inserting the Yuma Wash drainage area into five equations developed to estimate the magnitude of the 100-year discharge in Arizona or the southwest US (House and Baker, 2001) produces discharge values ranging from 14,900 to 38,900 m<sup>3</sup>/s. The 1997 flood along Yuma Wash is thus best described as a moderate flood.

At its headwaters, Yuma Wash has a relatively narrow valley (approximately 50 m wide) with a single dominant channel. The wash is incised into andesite and is laterally confined. Further downstream, valley width exceeds 450 m; and multiple braid channels are formed in sand and gravel. The outer edges of the braided channel pattern are defined by Holocene and Pleistocene terraces and have vertical or nearly vertical walls formed in moderately indurated alluvium. Vegetation cover in the upland areas of the drainage basin is 1–5%, but increases to an average of 31% within the wash itself. Dominant vegetation in the channels is composed of xeric woody species and phreatophytes such as ironwood (*Olneya tesota* Gray), blue palo verde (*Cercidium floridum* Benth.), mesquite (*Prosopis juliflora* (Swartz) DC), smoke-tree (*Dalea spinosa* Gray), and



Fig. 2. Photograph of Yuma Wash at the time of the resurvey. Note the linear bands of woody vegetation. Photo taken from the left of the river, looking upstream (person at bottom center for scale).

catclaw acacia (*Acacia greggii* Gray) (nomenclature follows Kearney and Peebles, 1964). Higher surfaces in the wash and uplands surrounding the wash are characterized by creosote bush (*Larrea tridentata* (DC) Coville), brittlebush (*Encelia farinosa* Gray), and a variety of cactus species. Clumps of vegetation occur in linear or lemniscate patterns defining depositional surfaces on the valley bottom and shallow interfluvies between braid channels (Fig. 2). The woody species growing on bars in and adjacent to active channels are resistant to removal by scour and are likewise adapted to survive flooding. Trunks of woody species tipped in a downstream direction, abrasion scars, sediment deposition around patches of vegetation, and piles of woody debris upstream of trunks were all common features in the wash.

The Yuma Wash drainage basin includes three large tributary basins: the East Fork (34 km<sup>2</sup>), the West Fork (43 km<sup>2</sup>), and the North Fork (43 km<sup>2</sup>) basins (Fig. 1). Reach-scale bed gradient averages 0.02 throughout the study area. The thalweg profile of Yuma Wash surveyed in 1995 is relatively constant, but does include minor variations associated with tributary confluences. A steeper reach below each confluence probably reflects increased discharge and transport capacity. This reach extends up to 600-m downstream from the confluence, with up to a meter of bed incision below the projected constant-grade thalweg line. Transmission losses farther downstream create a zone of aggradation downstream from this steeper reach. This zone extends up to a kilometer downstream and has up to a meter of bed aggradation above the projected thalweg line.

### 3. Methods

As part of the Legacy Resource Management Program, in 1995, the Department of Defense initiated a baseline study of the geological and biological resources within the Yuma Proving Ground. This included a geomorphic characterization of the Yuma Wash by Ayres Associates (1996) during which 22 cross-sections were surveyed and monumented along the wash. In January 1998, <6 months after Hurricane Nora, we resurveyed nine of these cross-sections along a 19-km reach of the wash (time limitations prevented us from resurveying more cross-sections).

No flows occurred between Hurricane Nora and our resurvey. We also established two detailed survey reaches for hydraulic modeling (Fig. 1): six cross-sections were surveyed approximately 2 km upstream from the most upstream of the resurveyed cross-sections in a stable, bedrock-controlled reach 100-m long; and five cross-sections were surveyed along a reach 400 m in length around a cross-section with lateral bedrock control. Surveying was conducted with a Topcon CTS-2 total station. Organic material and silt and fine sand deposits were used to define water-surface profiles for the Hurricane Nora flood; the top of each deposit was assumed to equal peak stage. Maximum depth of scour was estimated by measuring depth to a consolidated, resistant layer of caliche in the bed alluvium that would substantially impede bed erosion.

#### 3.1. Discharge estimation and downstream hydraulic geometry

The one-dimensional, step-backwater program HEC-RAS (HEC, 1996) was used to model flood hydraulics for the two detailed survey reaches. HEC-RAS uses the Bernoulli energy equation to route user-specified discharges through surveyed channel geometry. Resultant water-surface profiles are then matched to surveyed water-surface profiles in an iterative procedure until the discharge producing the best match is identified.

There are many limitations to the use of one-dimensional flow models for simulating flow in flashy streams with multiple flow paths. The energy equations used in the one-dimensional, step-backwater modeling are based on the assumption of steady, uniform flow. Flash flooding is by definition unsteady. Flash flood hydrographs often exhibit vertical or near-vertical rising limbs, indicating instantaneous change in discharge associated with a flood wave or flood bore (Schick, 1970). In order to minimize the error associated with violations of these assumptions, we selected straight reaches with relatively uniform channel geometry and lateral bedrock control and assumed that high-water marks represented a peak stage that could be modeled as steady uniform flow over a period of minutes. Discharge was also estimated using the Manning equation (slope-area method) for the two hydraulic model reaches.

Six high-water marks were used along the upstream detailed survey reach, and 33 along the downstream reach. Roughness coefficients for each reach were calculated using the additive method of Cowan (1956):

$$n = (n_b + n_1 + n_2 + n_3 + n_4)m$$

where  $n_b$  is a base value of  $n$  for straight, uniform, smooth channels in natural materials (0.012–0.07),  $n_1$  is a correction factor for the effect of surface irregularities (0–0.02),  $n_2$  is a value for variations in shape and size of the channel cross-section (0–0.015),  $n_3$  is a value for obstructions (0–0.05),  $n_4$  is a value for vegetation and flow conditions (0.002–0.1), and  $m$  is a value for meandering of the channel (1–1.3). Base values of  $n$  were estimated using the median grain size of the bed material and calculating grain roughness using an empirical equation developed by Strickler (1923):

$$n = 0.0151D_{50}^{1/6}$$

where  $D_{50}$  is median grain size in millimeter. The Strickler equation is recommended for use on coarse-bedded, dryland streams because it was developed using data from gravel-bed streams (Graf, 1988a). Field notes, photographs, and values calculated for other ephemeral streams in the region were all used in estimating  $n$  for Yuma Wash (Arcement and Schneider, 1987; Phillips and Ingersoll, 1998; Phillips et al., 1998). Sensitivity analyses were performed by adjusting  $n$  within a range of reasonable values ( $0.03 < n < 0.06$ ) and recording discharge for each step-backwater trial.

Peak flow was also estimated at each of the resurveyed cross-sections throughout the wash using slope-area calculations. Water-surface elevation was plotted at the level indicated by high-water marks at each cross-section. Maximum depth flow was estimated from pre-flood cross-sectional geometry, likely maximum scour depth as defined by the resistant layer in the channel bed, and post-flood high-water marks. Several hydraulic parameters (hydraulic or average depth, wetted perimeter, wetted cross-sectional area, and water-surface width) were measured from each cross-sectional plot using the hydraulics module of Scour and Fill, version 7.1 (USDI, 1995).

Estimated discharge from each cross-section was used to develop exponential power functions to evaluate downstream hydraulic geometry in Yuma Wash during the flood. For braided reaches, flow width was the sum of individual channel widths and did not include areas above high water.

### 3.2. Channel change

Channel change at each cross-section between the 1995 and 1998 surveys was quantified using four measures (USDI, 1995): area of cross-sectional scour ( $m^2$ ), area of cross-sectional fill ( $m^2$ ), net change in channel area ( $m^2$ ), and change in thalweg depth (m). Measures of channel change were obtained by overlaying 1995 and 1998 cross-sectional surveys in Scour and Fill, version 7.1 and measuring deviations from the 1995 baseline. Hydraulic variables (Table 2) were calculated from cross-sectional and water-surface data for each cross-section surveyed in 1995 and resurveyed in 1998. Physical characteristics (Table 3) were measured from survey data, field notes and photos, and 1:24,000-scale topographic maps. Rate of change

Table 2

Hydraulic variables measured from pre-hurricane cross-sectional geometry using the water-surface elevation at peak flow during Hurricane Nora flood along Yuma Wash; water-surface elevation was estimated using high-water marks at each resurveyed cross-section

Hydraulic variable	Units	Equation
Water-surface width, $W$	m	$\Sigma$ (water-surface width of subchannels)
Wetted perimeter, $P$	m	$\Sigma$ (wetted perimeter of subchannels)
Hydraulic depth, $D_h$	m	$D_h = A/W$
Wetted area of flow, $A$	$m^2$	$A = D_h W$
Maximum flow depth, $D_{mx}$	m	–
Hydraulic radius, $R_h$	no units	$R_h = A/WP$
Flow velocity, $V$	m/s	$V = (R_h^{0.67} s^{0.50})/n$ , where $s$ is the energy slope (approximated by water-surface slope) and $n$ is the hydraulic roughness coefficient
Discharge, $Q$	$m^3/s$	$Q = VA$
Shear stress, $\tau$	$N/m^2$	$\tau = \gamma R_h s$ , where $\gamma$ is the specific weight of water
Total stream power, $\Omega$	W/m	$\Omega = \gamma Qs$
Unit stream power, $\omega$	$W/m^2$	$\omega = \Omega/W$

Table 3  
Physical variables measured for each cross-section resurveyed along Yuma Wash

Physical variables	Units	Description
Drainage basin area	km <sup>2</sup>	drainage basin area above each cross-section
Distance downstream	km	distance downstream from the most upstream cross-section (25)
Valley width	m	valley width at the cross-section
Rate of change in valley width	m/m	the rate of change in valley width upstream from the cross-section; calculated by dividing the difference in valley width 200 m above the cross-section and at the cross-section by 200 m
Bedrock	–	binary variable; value of 1 if bedrock confinement was noted on at least one side of the channel at the cross-section, and 0 if bedrock was not present through the 200-m reach above the cross-section
Valley slope	m/m	bed slope through the reach 200 m upstream and downstream of the cross-section
Number of channels	–	number of channels and subchannels at a cross-section
Percent vegetation	%	percent of the cross-section width vegetated, estimated from oblique photographs

in valley width was calculated from measurements of valley width at the resurveyed cross-section and measurements of valley width 200 m upstream of the cross-section. These measures were taken from 1:24,000-scale topographic maps. Percent of the cross-section vegetated was estimated visually by examining the percentage of the cross-section occupied by woody plants. Bedrock confinement of the channel was a binary (dummy) variable: 1 if one or both sides of the valley was comprised of bedrock, 0 if bedrock was not exposed on either side of the valley.

Stepwise regression was used to determine which of the physical and hydraulic variables best explained the net change in cross-sectional dimensions associated with the Hurricane Nora flood. Spearman rank correlation was performed prior to regression model selection to eliminate collinearity between variables. Independent variables used in the correlation analysis are shown in Tables 2 and 3. After eliminating variables expressing collinearity (Table 6), the final list of variables used for model selection included

three hydraulic variables (wetted perimeter, maximum flow depth, and flow velocity) and all of the physical variables shown in Table 3 with the exception of distance downstream.  $p$ -value of 0.15 from an  $F$ -test of the significance of each variable for entry into the model was selected. The same significance level ( $p < 0.15$ ) was selected for a variable to remain in the model (SAS Institute, 1999).

Cross-sections were classified as either aggraded or degraded based on net change in channel geometry from pre- to post-hurricane surveys. Stepwise discriminant analysis was used to develop a function to categorize cross-sections as aggraded or degraded based on the physical attributes of the channel. Stepwise discriminant analysis was also performed using the hydraulic variables to categorize a reach as aggraded or degraded. Because of the limited number of observations (i.e. cross-sections used in the analysis ( $n = 9$ )), the final discriminant function was limited to only the two most significant quantitative variables in the stepwise analysis. An  $F$ -test significance level of  $p < 0.15$  from analysis of covariance was used for both entry of variables into the model and for a variable to remain in the model with each iteration of the stepwise model selection process. The set of variables used to make-up each class (aggraded or degraded) complied reasonably well with the assumptions of multivariate normality with a common covariance matrix (SAS Institute, 1999). SAS/STAT, version 8 was used for all statistical analyses (SAS Institute, 1999).

## 4. Results

### 4.1. Discharge estimation and downstream hydraulic geometry

Calculated hydraulic data for the nine resurveyed cross-sections are summarized in Table 4. Slope-area estimates of discharge during Hurricane Nora compared well with estimates from the detailed study reaches developed with step-backwater methods. Both datasets indicate an uneven rate of downstream increase in discharge (Fig. 3), probably associated with variation in the magnitude and intensity of contributing flows from each of the subbasins of the wash. Ignoring inputs from slope runoff and minor

Table 4

Physical data and selected computed hydraulic data for resurveyed cross-sections along Yuma Wash

XS	Drainage area (km <sup>2</sup> )	Distance downstream (km)	Valley width (m)	Rate of change in valley width	Bedrock	Slope (m/m)	No. of channels	Percent coverage of vegetation, $D_{50}$ (mm)	Width (m)	Hydraulic depth (m)	Velocity (m/s)	Discharge (m <sup>3</sup> /s)
25	8.5	0.0	162	-0.08	1	0.023	3	22, 5	47	0.42	1.88	37
23	8.9	1.4	159	-0.36	0	0.023	4	67, 3	77	0.21	1.18	19
21	15.8	3.1	170	-0.11	1	0.021	5	38, 3	91	0.36	1.16	16
18	62.7	5.7	158	-0.47	1	0.019	4	30, 3.7	94	0.39	1.60	58
14	101.6	9.6	299	0.10	0	0.019	4	26, 1.9	108	0.39	1.65	71
11	105.6	11.7	130	0.29	0	0.019	5	18, 3	108	0.37	1.54	61
4	174.0	16.1	205	0.24	1	0.019	7	28, 1	198	0.53	1.98	210
2	180.1	18.2	453	0.19	0	0.020	9	24, 0.25	178	0.48	1.88	161
1	186.2	19.2	399	0.12	1	0.020	8	27, 0.06	377	0.38	1.66	237

tributaries, the discharge estimates suggest that the North Fork basin, which enters the wash downstream of the cross-section at 5.1 km, contributed approximately 41 m<sup>3</sup>/s (unit discharge of 0.95 m<sup>3</sup>/s/km<sup>2</sup>). The East Fork basin, which enters the main stem of the wash below the cross-section at 7.7 km, contributed approximately 12 m<sup>3</sup>/s (unit discharge of 0.35 m<sup>3</sup>/s/km<sup>2</sup>). The West Fork basin, which enters the main stem immediately downstream of the cross-section at 13.7 km, contributed approximately 149 m<sup>3</sup>/s (unit discharge of 3.46 m<sup>3</sup>/s/km<sup>2</sup>). The variability in the contribution of flow from the subbasins to the

main stem is likely a function of the spatial variability in the intensity of precipitation during the hurricane rather than a function of differences in contributing drainage basin area.

After plotting the high-water marks and reviewing the field notes, we discerned two distinct sets of high-water marks throughout the wash. A group of older high-water marks deposited 20–105 cm above the more recent deposits associated with Hurricane Nora provided evidence of a significantly larger flood. Discharge of this older flow was estimated for comparison with the Hurricane Nora flood using step-

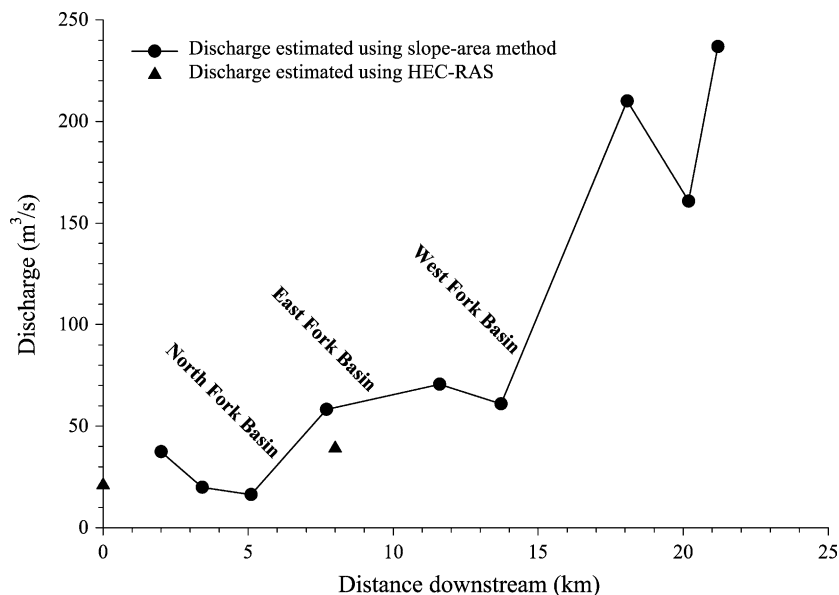


Fig. 3. Maximum discharge as a function of distance downstream during Hurricane Nora flood, as calculated from slope-area and step-backwater estimates. Approximate locations of confluences with subbasins of Yuma Wash are indicated.

backwater modeling and the slope-area method at the detailed survey reaches and the slope-area method for all other resurveyed cross-sections. Roughness values were held constant over the range of river stages.

Precisely dating these deposits was impractical, but precipitation data from the weather station at Yuma Proving Ground indicated that the three largest storms on record occurred in 1963, 1972, and 1989 (NOAA, 1998). Considering the relative magnitude, precipitation on previous days, and estimated age of the flood deposits, we infer that the older high-water marks noted in this study were deposited during flooding associated with a frontal storm system (76-mm precipitation) on 6 October 1972. Estimated discharge using the modeled water-surface elevation for this flood indicates a maximum peak value of  $1280 \text{ m}^3/\text{s}$  at the cross-section furthest downstream in the wash. This value falls on the regional envelope curve of maximum peak discharges calculated for ephemeral streams throughout the lower Colorado River basin

(House, 1997), and thus provides a reasonable magnitude for the probable maximum flood along Yuma Wash (Fig. 4).

Fig. 5 summarizes downstream hydraulic geometry relations for Yuma Wash. Examining the hydraulic geometry of ephemeral channels in the southwest US, Leopold and Miller (1956) found that the downstream increase along ephemeral channels is approximately the same for width, less for depth, and greater for velocity than average values for perennial rivers. They attributed these differences to the downstream increase in suspended-sediment concentration, which would dampen both turbulence and bed erosion. Along Yuma Wash, width increases substantially downstream, depth has a lesser increase than average river values, and the rate of velocity increase downstream is about average. The downstream increase in width may be attributed to the composition of the bed and bank material, which has less than 3% silt and clay. The only factor providing bank cohesion and flow resistance along Yuma Wash is

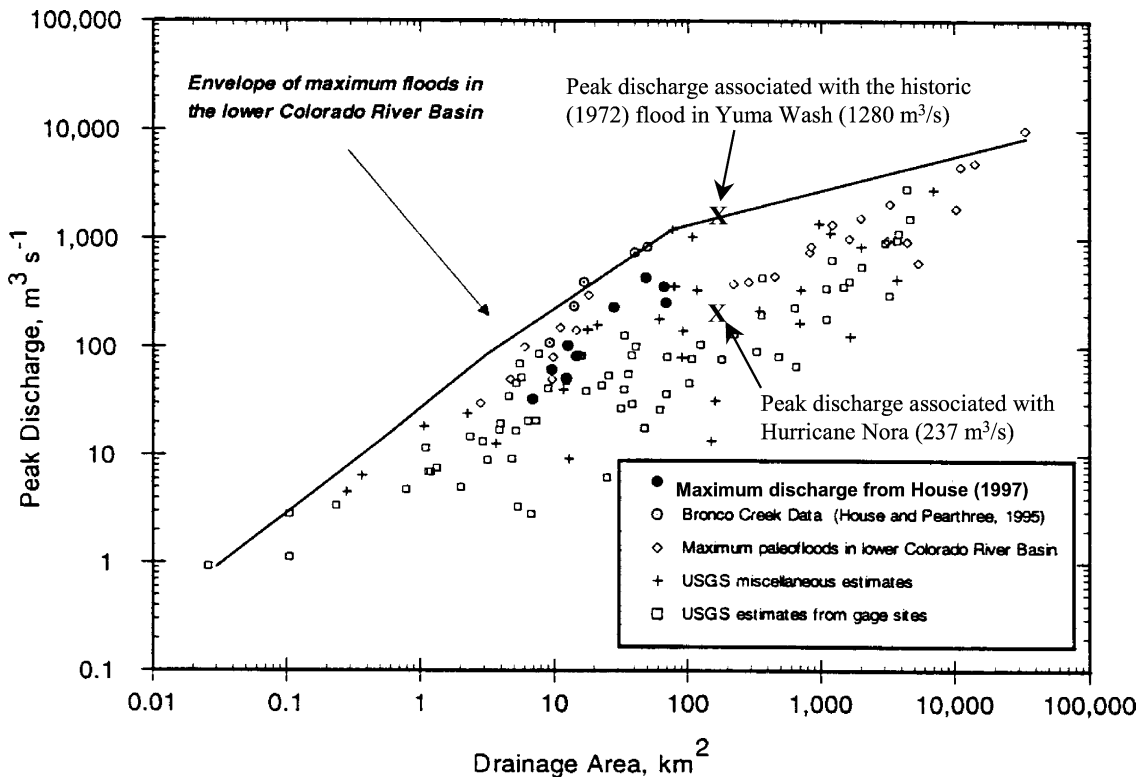


Fig. 4. Comparison of the maximum peak discharge for a historic flood in Yuma Wash and the Hurricane Nora flood to the regional envelope curve of maximum peak discharges versus drainage area in the lower Colorado River basin (from House, 1997).

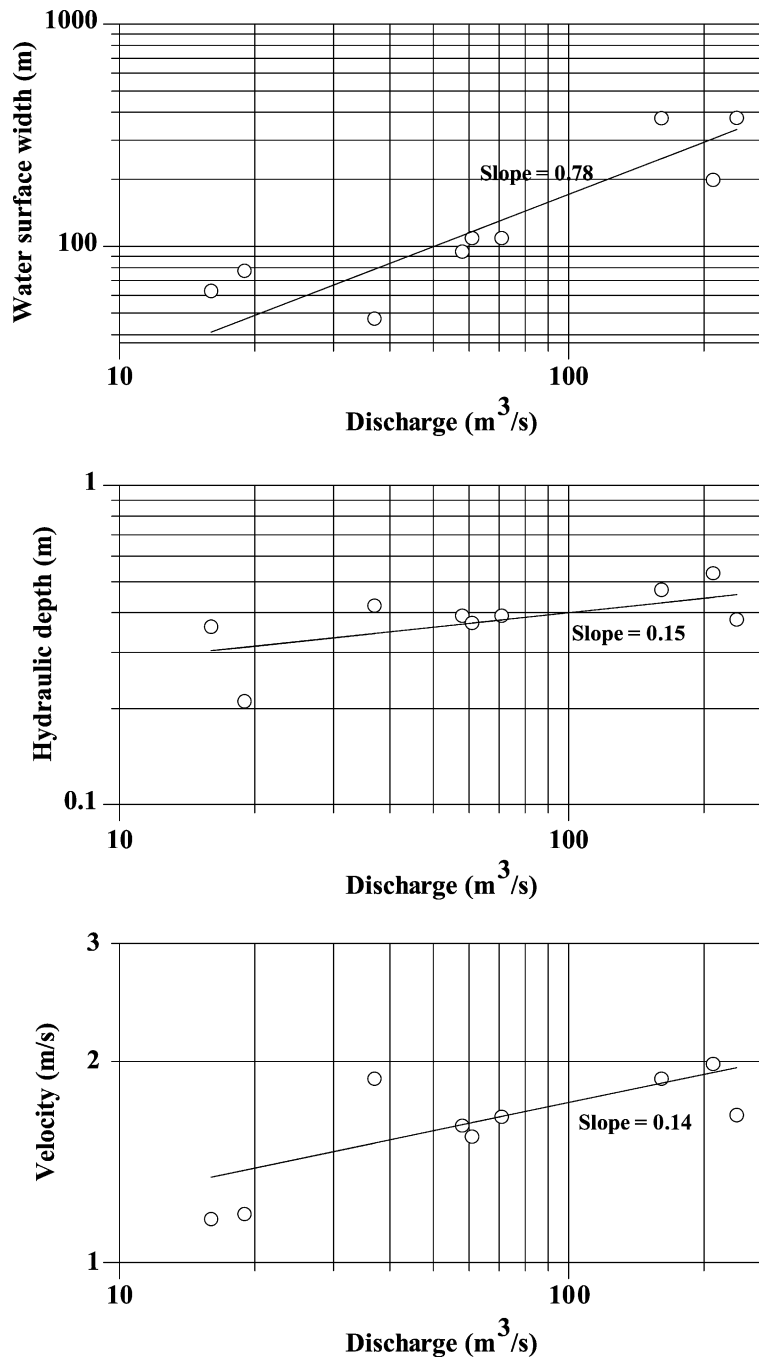


Fig. 5. Downstream hydraulic geometry relations in Yuma Wash during the Hurricane Nora flood.

vegetation, but this is apparently not sufficient to prevent bank erosion and formation of braid channels because of the unconsolidated nature of the coarse

gravel-bed material. Depth adjustments to increased discharge may not occur because channel width absorbs most of the downstream change. The vegeta-

tion, by substantially increasing channel boundary roughness, may also limit the rate of downstream increase in velocity.

#### 4.2. Channel change

Six of the nine resurveyed cross-sections along Yuma Wash experienced net bed aggradation (net fill), and three cross-sections had net degradation (net scour) (Fig. 6). Average net change of aggrading cross-sections was  $12.1 \text{ m}^2$  (S.E. =  $\pm 4.5 \text{ m}^2$ ), whereas the average net change of degrading cross-sections was  $-5.8 \text{ m}^2$  (S.E. =  $\pm 2.3 \text{ m}^2$ ). Average thalweg change was consistent with this trend; increase in thalweg elevation occurred at cross-sections that aggraded, and the thalweg typically scoured at cross-sections that experienced net scour.

In general, cross-section net aggradation and thalweg aggradation occurred along wider valley reaches and where channels and subchannels were more numerous, and net scour and thalweg scour were greater where the valley was narrower and flow was confined to fewer channels. Net fill was considerably higher in cross-sections furthest downstream in the wash. Net scour was greatest at intermediate distances downstream. Over the length of the wash resurveyed, degrading reaches alternated with aggrading reaches (Fig. 6). Patterns of aggradation and degradation suggest a wave-like movement of sediment through

the 19.2-km reach surveyed. These patterns could be attributed to an event-driven, pulsed movement of sediment through the wash. Alternatively, the observed patterns may have been influenced by the balance between water and sediment discharge from tributary inflows of the subbasins of the wash. The North Fork and East Fork junctions are not associated with substantial changes in net fill, but the fill does increase dramatically downstream from the West Fork junction. The West Fork had a unit discharge several times that of the North Fork and East Fork, suggesting much greater sediment transport capacity in the West Fork. As the flood flow from the West Fork spread across the main wash below the junction, channel fill would be expected.

A threshold response may also account for the observed net fill at some cross-sections. It is possible that discharge must attain some sufficient threshold volume to overtop in-channel bars that separate individual braided-flow paths. At lower discharges, flow is confined to deep, unvegetated, swifter flowing channels, resulting in scour. At higher discharges, stage is sufficient to overtop vegetated bars. Flow velocity decreases over bars because of higher roughness, which facilitates sediment deposition on the lee sides of stems (Nepf, 1999). Secondary flow cells in channels between bars may facilitate scouring and maintenance of unvegetated channels between vegetated islands (Graeme and Dunkerley, 1993; Wende

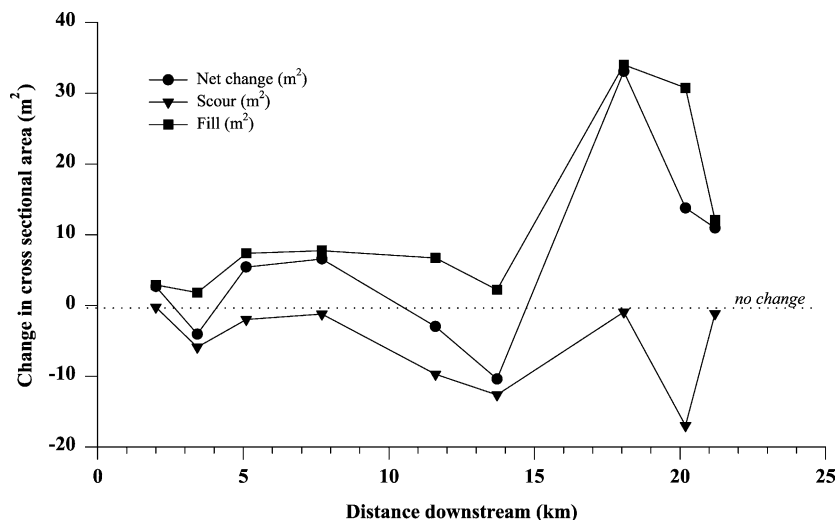


Fig. 6. Changes in channel geometry of Yuma Wash from cross-sectional surveys measured prior to and following Hurricane Nora flooding.

and Nanson, 1998). These secondary flow cells, which scour sediment from channels and deposit sediment on bars, may produce regularly spaced bar and channel sequences in braided streams such as Yuma Wash. Linear bands of vegetation oriented downstream were evident at many of the resurveyed cross-sections in the wash (Fig. 2).

Multiple regression model selection indicates that the number of channels at a particular cross-section, the channel slope, whether the channel is confined on one or both sides by bedrock, and the percent of the cross-section occupied by woody plants are the most important of the physical channel characteristics in determining the degree and direction of channel

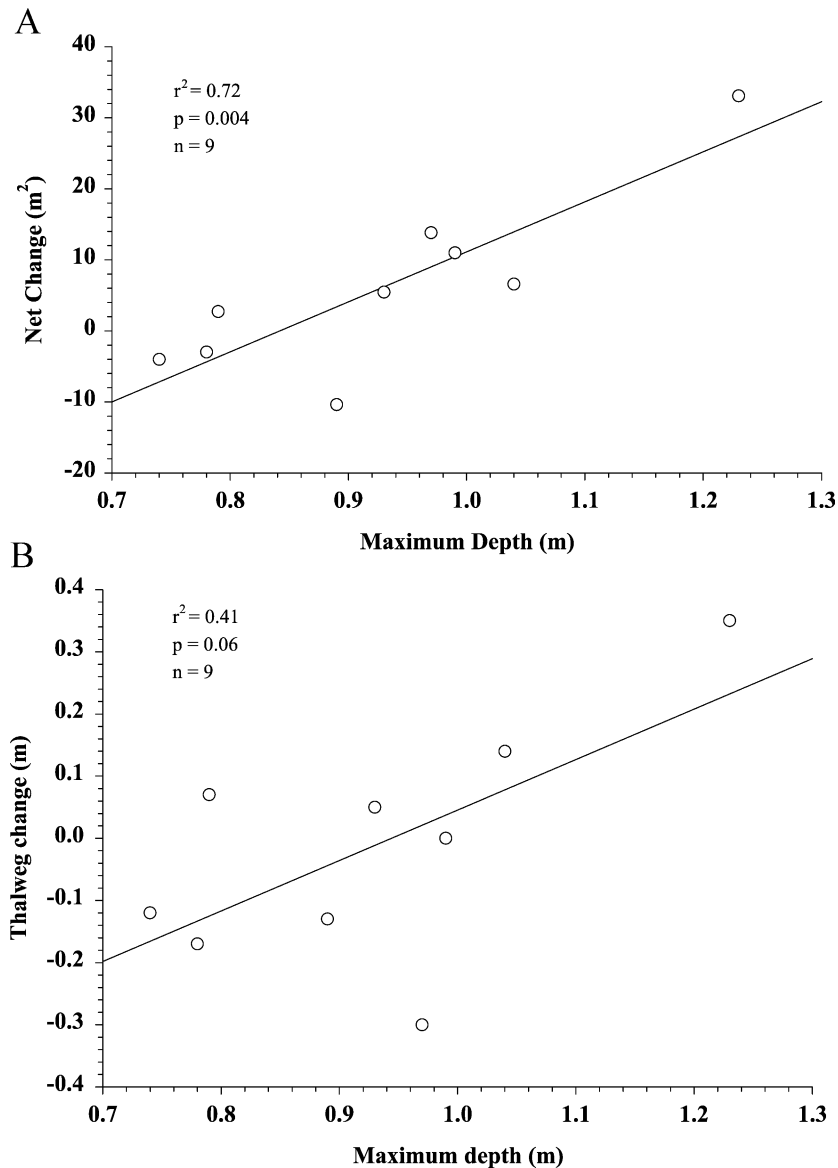


Fig. 7. (A) Net change in channel bed elevation plotted as a function of maximum depth of flow for Yuma Wash. (B) Change in thalweg elevation plotted as a function of maximum depth of flow for Yuma Wash.

change. The most important hydraulic attribute at high flow during Hurricane Nora rainfall was maximum depth of flow. Models containing combinations of these variables explained from 36% to 96% of the variability in the thalweg change, net change, scour, and fill (Fig. 7, Table 6). Thalweg scour was inversely related to depth of flow and diminished with increasing number of channels in a cross-section (along wider valley bottoms; Tables 5 and 6). Cross-sections with smaller maximum flow depths and those confined to fewer channels tended to have higher thalweg scour, supporting the concept of a threshold discharge. Discharges below this threshold are confined to low-flow channels which are scoured; discharges sufficient to overtop vegetated bars enable sediment transported by saltation and in suspension to be deposited on the tops, margins, and downstream ends of these bars. The linear relationship between maximum depth and cross-section fill ( $R^2 = 0.36$ ;  $p = 0.0514$ ) and the negative relationship between scour and percent vegetation ( $R^2 = 0.96$ ,  $p = 0.0001$ ) both provide evidence of the threshold response between discharge and channel response (Table 6).

Stepwise discriminant analysis of cross-section attributes resulted in the selection of two variables that best categorize cross-sections into classes: valley width and number of channels and subchannels. The discriminant function containing these two variables that characterize the cross-section correctly categorized 67% of resurveyed cross-sections as aggraded or degraded (Wilks' Lambda  $F_{6,8} = 8.33$ ,  $p = 0.0043$ ). In general, the discriminant function based on cross-section attributes classified cross-sections with wider valleys and numerous multiple channels as aggraded. Cross-sections in narrower valleys with fewer channels were classified as degraded. Stepwise discriminant function analysis using hydraulic characteristics resulted in a robust discriminant function (Wilks' lambda  $F_{1,7} = 4.28$ ,  $p = 0.0775$ ), with only one misclassification. One variable, maximum depth of flow, was selected over all other variables for the final discriminant function. The function containing maximum depth correctly classified eight of the nine resurveyed cross-sections, indicating generally that cross-sections with greater maximum flow depth aggrade, whereas those with lower flow depths degrade. Flow depth is a function of cross-sectional

Table 5  
Correlation matrices showing the correlation coefficient from Spearman rank correlations for hydraulic variables (top table) and physical variables (lower table) used in the analyses

Hydraulic variables	<i>W</i>	<i>P</i>	<i>D<sub>h</sub></i>	<i>A</i>	<i>D<sub>mx</sub></i>	<i>R<sub>h</sub></i>	<i>V</i>	<i>Q</i>	$\tau$	$\Omega$
Water surface width, <i>W</i>	1.00	*	*	*	*	*	*	*	*	*
Wetted perimeter, <i>P</i>	<b>0.97</b>	1.00	*	*	*	*	*	*	*	*
Hydraulic depth, <i>D<sub>h</sub></i>	0.40	0.34	1.00	*	*	*	*	*	*	*
Wetted area of flow, <i>A</i>	<b>0.93</b>	<b>0.93</b>	0.57	1.00	*	*	*	*	*	*
Maximum flow depth, <i>D<sub>mx</sub></i>	0.60	0.57	0.52	0.53	1.00	*	*	*	*	*
Hydraulic radius, <i>R<sub>h</sub></i>	0.46	0.39	<b>0.99</b>	0.63	0.46	1.00	*	*	*	*
Flow velocity, <i>V</i>	0.53	0.52	<b>0.93</b>	<b>0.73</b>	0.47	<b>0.95</b>	1.00	*	*	*
Discharge, <i>Q</i>	<b>0.93</b>	<b>0.93</b>	0.57	<b>0.99</b>	0.53	0.63	<i>0.73</i>	1.00	*	*
Shear stress, $\tau$	0.43	0.42	<b>0.91</b>	<i>0.66</i>	0.42	<b>0.94</b>	<b>0.98</b>	<i>0.67</i>	1.00	*
Total stream power, $\Omega$	<b>0.93</b>	<b>0.93</b>	0.57	<b>0.99</b>	0.53	0.63	<i>0.73</i>	<b>0.99</b>	<i>0.67</i>	1.00
Unit stream power, $\omega$	0.30	0.28	<b>0.86</b>	0.57	0.27	<b>0.89</b>	<b>0.93</b>	0.57	<b>0.95</b>	0.57

Physical variables	DA	<i>D</i>	VW	CH VW	BR	SLOPE	#CHAN
Drainage basin area, DA	1.00	*	*	*	*	*	*
Distance downstream, <i>D</i>	<b>0.99</b>	1.00	*	*	*	*	*
Valley width, VW	0.58	<b>0.88</b>	1.00	*	*	*	*
Rate change VW, CH VW	<i>0.68</i>	<i>0.68</i>	0.28	1.00	*	*	*
Bedrock, BR	-0.09	-0.09	0.00	-0.25	1.00	*	*
Valley slope, SLOPE	-0.58	-0.58	-0.05	-0.57	0.17	1.00	*
Number of channels, #CHAN	<b>0.88</b>	<b>0.88</b>	0.60	0.61	-0.04	-0.35	1.00
Percent vegetated, % VEG	-0.27	-0.27	-0.07	-0.67	0.26	0.21	-0.08

Italics indicates significance at  $p < 0.05$ ; bold italics indicates significance at  $p < 0.01$ .

Table 6  
Model parameters, adjusted  $R^2$  values, and  $p$ -values

Model	Adjusted $R^2$	$p$ -value
Thalweg change = $-0.89 + 1.36$ (maximum depth) $- 0.07$ (number of channels)	0.80	0.0081
Net channel change = $-132.9 + 88.64$ (maximum depth) $+ 2820.27$ (slope)	0.82	0.0063
Scour = $-0.11 + 0.087$ (bedrock) $+ 0.046$ (percent vegetation)	0.96	0.0001
Fill = $-0.15 + 0.25$ (maximum depth)	0.36	0.0514

Variables included in the models were selected using stepwise regression. Units for variables are shown in Tables 2 and 3.

geometry, discharge, and boundary roughness. During Hurricane Nora, hydraulic depth increased with distance downstream at an exponential rate of 0.15.

The observed statistical relationships may be explained as follows. Higher flow volumes facilitate the flooding of depositional bars located in areas of energy dissipation. In these areas, shear stress is lower than within deeper portions of the channel, and vegetation may become established. The presence of vegetation and the shallower flow depths over these features increase the hydraulic roughness of the surface. The decrease in flow velocity caused by increased hydraulic roughness from plant stems may substantially decrease the sediment transport capacity of the flow, even during relatively high flows (Nepf, 1999). At lower discharges, when flow is confined to multiple channels, interchannel bar growth cannot occur through vertical accretion. Therefore, high flows (above the overbank threshold) are necessary for substantial net aggradation of cross-sections to occur.

Given a water-surface level related to some discharge at a particular cross-section, the width of the valley, and the number of channels conducting flow, the discriminant function has an acceptable ability to predict whether the cross-section will aggrade or degrade. The quantity of net scour or fill was also found to be a function of maximum depth of flow. In regression analyses, maximum flow depth explains 72% of the variability of scour or fill measured in Yuma Wash ( $R^2 = 0.72$ ;  $p = 0.004$ ) (Fig. 7A). Discharge was greatest at the lowest three cross-sections in the wash, and depth of flow was greatest at these cross-sections as well.

## 5. Discussion and conclusions

The analysis of channel change during the 1997 Hurricane Nora flood along Yuma Wash provides

some insight into the factors influencing downstream hydraulic geometry and channel adjustment along ephemeral streams. Proceeding downstream along Yuma Wash, channel boundary resistance decreases as bedrock gives way to alluvium along the banks and the channel-bed material becomes slightly finer grained. Valley width does not increase uniformly downstream. Whether this results from geologic controls or some other factor, changes in valley width create a framework within which channel adjustment occurs via the number of subchannels, percent vegetation cover, and flow width and depth. During moderate floods such as that in 1997, discharge increases downstream. The combination of increasing discharge and decreasing boundary resistance produces a braided channel pattern where vegetated bars provide local roughness and erosional resistance. Where wider valley reaches and more numerous channels allow more vegetated bars to form, aggradation occurs during high flows. Aggradation is greatest where flow depth is sufficiently high to flood vegetated bars. Where flow is confined to subchannels, the cross-section scours. The presence of vegetated bars between subchannels in braided reaches thus creates a threshold effect with respect to flow depth versus net channel change.

Yuma Wash provides an interesting comparison to previous studies of downstream hydraulic geometry and channel change during floods along ephemeral rivers in that the 1997 flood discharge increased downstream, and the channels of the drainage system have partial lateral control rather than being completely alluvial. The downstream increase in discharge, combined with the lack of cohesion in channel-margin sediments and the decreasing lateral confinement downstream, probably explains the rapid increase of channel width downstream, relative to rates of change in channel width described in previous studies (e.g. Leopold and Miller, 1956). At smaller spatial scales,

characteristics such as valley width and gradient, and number of braid channels and vegetation, correlate well with channel change between 1995 and 1998.

The cross-sectional changes inferred to result from the 1997 flood along Yuma Wash are modest compared to published studies of major floods along ephemeral channels (Tooth, 2000). Such studies have documented a variety of channel responses, including pattern changes (Graf, 1988a), substantial widening (Burkham, 1972; Osterkamp and Costa, 1987; Kresan, 1988) and lateral migration (Graf, 1983b), entrenchment (Graf, 1983a), and floodplain erosion and deposition (Wells, 1990; Zawada and Smith, 1991). The modest changes along Yuma Wash presumably result from the moderate discharge of the 1997 flood, and may also relate to the occurrence of a flood approximately five times larger in 1972. We have insufficient evidence to estimate the magnitude or spatial patterns of channel change during the 1972 flood, but there is no reason to assume that the basic patterns of channel change differed in kind from those inferred to have occurred during the 1997 flood. The 1972 flood may have shaped the geomorphic framework (valley width and gradient, number of subchannels) within which the 1997 flood occurred, but we cannot directly test this idea.

## Acknowledgements

This study was funded by the US Army Research Office, Department of Defense, under the Legacy Resource Management Program (Grant Number DAAG55-98-1-0037). We thank Russell Harmon of the Army Research Office for suggesting the project, Valerie Morrill and Jody Latimer of the Yuma Proving Ground for assisting with the field work, John Stednick for providing unpublished meteorological data for the 1997 storm, and Ayres Associates for providing access to their project report. Gregory Springer, Stephen Tooth, and Gerald Nanson provided very helpful review comments on the manuscript.

## References

- Arcement, G.J., Schneider, V.R., 1987. Roughness Coefficients for Densely Vegetated Flood Plains. US Geological Survey Water-Resources Investigations Report WRI 83-4247, Washington, DC, 62 pp.
- Ayres Associates, 1996. Geomorphic, hydrologic, and vegetation base-line conditions of Yuma Wash, Yuma Proving Grounds, Arizona. Unpublished report prepared for Waterways Experiment Station, US Army Corps of Engineers, Vicksburg, MS.
- Baker, V.R., 1977. Stream-channel response to floods, with examples from central Texas. *Geological Society of America Bulletin* 88, 1057–1071.
- Begin, Z.B., Inbar, M., 1984. Relationship between flows and sediment size in some gravel streams of the arid Negev, Israel. In: Koster, E.H., Steel, R.J. (Eds.), *Sedimentology of Gravels and Conglomerates*, vol. 10. Canadian Society of Petroleum Geologists, Calgary, Canada, pp. 69–75. Memoir.
- Burkham, D.E., 1972. Channel changes of the Gila River in Safford Valley, Arizona 1846–1970. US Geological Survey Professional Paper 655-G, Washington, DC.
- Cowan, W.L., 1956. Estimating hydraulic roughness coefficients. *Agricultural Engineering* 37, 473–475.
- Dunkerley, D.L., 1992. Channel geometry, bed material and inferred flow conditions in ephemeral stream systems, Barrier Range, western N.S.W., Australia. *Hydrological Processes* 6, 417–433.
- Graeme, D., Dunkerley, D.L., 1993. Hydraulic resistance by the river red gum, *Eucalyptus camaldulensis*, in ephemeral desert streams. *Australian Geographical Studies* 31, 141–154.
- Graf, W.L., 1978. Fluvial adjustments to the spread of tamarisk in the Colorado Plateau region. *Geological Society of America Bulletin* 89, 1491–1501.
- Graf, W.L., 1983a. Downstream changes in stream power in the Henry Mountains region, Utah. *Annals of the Association of American Geographers* 73, 373–387.
- Graf, W.L., 1983b. Flood-related channel change in an arid region river. *Earth Surface Processes and Landforms* 8, 125–139.
- Graf, W.L., 1988a. *Fluvial Processes in Dryland Rivers* Springer, Berlin.
- Graf, W.L., 1988b. Definition of flood plains along arid-region rivers. In: Baker, V.R., Kochel, R.C., Patton, P.C. (Eds.), *Flood Geomorphology*. Wiley, New York, pp. 231–242.
- House, P.K., 1997. An Unconventional, Multidisciplinary Approach to Evaluating the Magnitude and Frequency of Flash Floods in Small Desert Watersheds. Arizona Geological Survey Open-File Report 97-9, 46 pp.
- House, P.K., Baker, V.R., 2001. Paleohydrology of flash floods in small desert watersheds in western Arizona. *Water Resources Research* 37, 1825–1839.
- Hydrologic Engineering Center (HEC), 1996. HEC-RAS River Analysis System version 1.1 software. Developed by US Army Corps of Engineers, Hydrologic Engineering Center, Davis, CA.
- Kearney, T.H., Peebles, R.H., 1964. *Arizona Flora* University of California Press, Los Angeles, CA.
- Knighton, D., 1998. *Fluvial Forms and Processes: A New Perspective*. Arnold, London. 383 pp.
- Kochel, R.C., 1988. Geomorphic impact of large floods: review and new perspectives on magnitude and frequency. In: Baker, V.R., Kochel, R.C., Patton, P.C. (Eds.), *Flood Geomorphology*. Wiley, New York, pp. 169–187.

- Kresan, P.L., 1988. The Tucson, Arizona flood of October 1983. In: Baker, V.R., Kochel, R.C., Patton, P.C. (Eds.), *Flood Geomorphology*. Wiley, New York, pp. 465–489.
- Leopold, L.B., Miller, J.P., 1956. Ephemeral Streams—Hydraulic Factors and their Relation to the Drainage Net: Physiographic and Hydraulic Studies of Rivers. US Geological Survey Professional Paper 282-A, 34 pp.
- Leopold, L.B., Wolman, M.G., Miller, J.P., 1964. *Fluvial Processes in Geomorphology*. Freeman, San Francisco, CA. 522 pp.
- Mabbutt, J.A., 1977. *Desert Landforms*. Australian National Univ. Press, Canberra.
- Nepf, H.M., 1999. Drag, turbulence, and diffusion through emergent vegetation. *Water Resources Research* 35, 479–489.
- NOAA, 1998. National Oceanic and Atmospheric Administration NCDC Summary of the Day Weather Data. EarthInfo, Boulder, CO.
- Osterkamp, W.R., 1980. Sediment-morphology relations of alluvial channels. Proceedings of the Symposium on Watershed Management. American Society of Civil Engineers, New York, pp. 188–199.
- Osterkamp, W.R., Costa, J.E., 1987. Changes accompanying an extraordinary flood on a sand-bed stream. In: Mayer, L., Nash, D. (Eds.), *Catastrophic Flooding*. Binghamton Symposium in Geomorphology, vol. 18. Allen & Unwin, Boston, pp. 201–224.
- Park, C.C., 1977. World-wide variations in hydraulic geometry exponents of stream channels: an analysis and some observations. *Journal of Hydrology* 33, 133–146.
- Phillips, J.V., Ingersoll, T.L., 1998. Verification of Roughness Coefficients for Selected Natural and Constructed Stream Channels in Arizona. US Geological Survey Professional Paper 1584, Washington, DC, 77 pp.
- Phillips, J.V., McDoniel, D., Capesius, J.P., Asquith, W., 1998. Method to Estimate Effects of Flow-Induced Vegetation Changes on Channel Conveyances of Streams in Central Arizona. US Geological Survey Water-Resources Investigations Report 98-4040, Washington, DC, 43 pp.
- Reid, I., Laronne, J.B., 1995. Bed load sediment transport in an ephemeral stream and a comparison with seasonal and perennial counterparts. *Water Resources Research* 31, 773–781.
- SAS Institute, 1999. SAS/STAT User's Guide, Version 8. SAS Institute, Cary, NC.
- Schick, A.P., 1970. Desert floods-interim results of observations in the Nahal Yael research watershed, southern Israel, 1965–1970. IAHS-UNESCO Symposium on the Results of Research on Representative and Experimental Basins, Wellington, NZ.
- Strickler, A., 1923. Beitrage zur Frage der Geschwindigkeitsformel und der Rauheitszahlen fur Strome, Kanale und geschlossene Leitungen. Mitt Eidigen Amt Wasserwirtsch, Bern.
- Thornes, J.B., 1977. Channel changes in ephemeral streams: observations, problems and models. In: Gregory, K.J. (Ed.), *River Channel Changes*. Wiley, Chichester, pp. 317–335.
- Tooth, S., 1999a. Floodouts in central Australia. In: Miller, A.J., Gupta, A. (Eds.), *Varieties of Fluvial Form*. Wiley, Chichester, pp. 219–247.
- Tooth, S., 1999b. Downstream changes in floodplain character on the Northern Plains of arid central Australia. In: Smith, N.D., Rogers, J. (Eds.), *Fluvial Sedimentology VI*. International Association of Sedimentologists, Special Publication, vol. 28. Blackwell, Oxford, pp. 93–112.
- Tooth, S., 2000. Process, form and change in dryland rivers: a review of recent research. *Earth-Science Reviews* 51, 67–107.
- Tooth, S., Nanson, G.C., 1999. Anabranching rivers on the Northern Plains of arid central Australia. *Geomorphology* 29, 211–233.
- Tooth, S., Nanson, G.C., 2000. Equilibrium and nonequilibrium conditions in dryland rivers. *Physical Geography* 21, 183–211.
- USDI, 1995. Scour and Fill Version 7.1 Software. US Department of the Interior, National Biological Service, Arcata, CA.
- Wells, L.E., 1990. Holocene history of the El Nino phenomenon as recorded in flood sediments of northern coastal Peru. *Geology* 18, 1134–1137.
- Wende, R., Nanson, G.C., 1998. Anabranching rivers: ridge-form alluvial channels in tropical northern Australia. *Geomorphology* 22, 205–224.
- Wilson, E.D., 1960. *Geologic Map of Yuma County, Arizona*. Arizona Bureau of Mines, University of Arizona, Tucson.
- Wohl, E.E., Greenbaum, N., Schick, A.P., Baker, V.R., 1994. Controls on bedrock channel incision along Nahal Paran, Israel. *Earth Surface Processes and Landforms* 19, 1–13.
- Wolman, M.G., Gerson, R., 1978. Relative scales of time and effectiveness of climate in watershed geomorphology. *Earth Surface Processes and Landforms* 3, 189–208.
- Zawada, P.K., Smith, A.M., 1991. The 1988 Orange River flood, Upington region, Northwestern Cape Province, RSA. *Terra Nova* 3, 317–324.